

Carbon-Bridged Oligo(phenylenevinylene)s: Stable π -Systems with High Responsiveness to Doping and Excitation

Xiaozhang Zhu,^{†,||} Hayato Tsuji,^{*,†,‡} Juan T. López Navarrete,[§] Juan Casado,[§] and Eiichi Nakamura^{*,†}

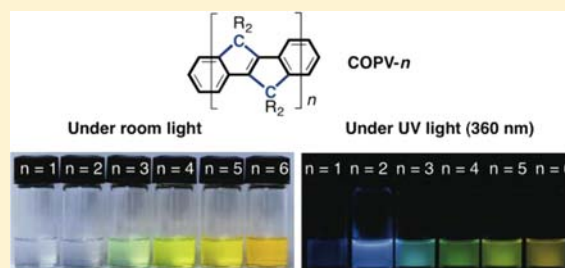
[†]Department of Chemistry, School of Science, The University of Tokyo, Hongo, Bunkyo-ku, Tokyo 113-0033, Japan

[‡]JST-PRESTO, 4-1-8 Honcho, Kawaguchi, Saitama 332-0012, Japan

[§]Department of Physical Chemistry, University of Málaga, Campus de Teatinos s/n, Málaga 29071, Spain

Supporting Information

ABSTRACT: The high responsiveness of π -conjugated materials to external stimuli, such as electrons and photons, accounts for both their utility in optoelectronic applications and their chemical instability. Extensive studies on heteroatom-stabilized π -conjugated systems notwithstanding, it is still difficult to combine high performance and stability. We report here that carbon-bridged oligo(*p*-phenylenevinylene)s (COPV-*n*) are not only more responsive to doping and photoexcitation but also more stable than the conventional *p*-phenylenevinylenes and poly(3-hexylthiophene), surviving photolysis very well in air, suggesting that they could serve as building blocks for optoelectronic applications. Activation of the ground state by installation of bond angle strain toward the doped or photoexcited state and the flat, rigid, and hindered structure endows COPVs with stimuli-responsiveness and stability without recourse to heteroatoms. For example, COPV-6 can be doped with an extremely small reorganization energy and form a bipolaron delocalized over the entire π -conjugated system. Applications to bulk and molecular optoelectronic devices are foreseen.



INTRODUCTION

One major concern in the practical application of organic optoelectronic devices is the stability of the π -conjugated organic materials against heat, light, and oxygen. Because the responsiveness of π -systems to external stimuli inevitably generates chemically reactive species, such as radical cations, radical anions, and photoexcited states, high stimuli-responsiveness and high chemical stability of organic materials appear to be fundamentally incompatible. One common strategy to solve this problem is to stabilize the π -system with heteroatoms;¹ however, this strategy is not necessarily ideal because the polarized carbon–heteroatom bonds localize polarons and excitons in the molecule and create new decomposition pathways. For example, heteroatom stabilization of otherwise unstable poly(*p*-phenylenevinylene)s (PPVs) and oligo(PV)s (OPVs) has led to the dramatic development of new research areas.² However, these compounds are structurally flexible and are not sufficiently responsive to doping and photoexcitation nor are they stable under ambient conditions or in the doped and photoexcited states.³ To reconcile performance and stability, we decided to eliminate entirely heteroatoms from the π -system and implement a structural feature that can stabilize the doped and excited states. We tested our idea on a PV monomer and a dimer (COPV-1 and -2 in Figure 1a), in which we buttressed the σ -framework of a PV unit with one-carbon bridges and found that they exhibit ambipolar carrier mobilities of $5\text{--}6 \times 10^{-3} \text{ cm}^2/\text{V s}$ for both hole and electron,⁴ a value close to the upper limit for amorphous materials. In

addition, COPV-1 was found to serve as an effective molecular wire in a metal-free sensitizer in dye-sensitized solar cells (DSSCs), which recorded among the highest open-circuit voltage and power conversion efficiency for metal-free dyes.⁵ Being aware that doping and photoexcitation weaken the vinylenic bonds in PPVs, we surmised that it is the ring strain of the bicyclo[3.3.0]octatriene σ -framework that increased the materials' performance. To validate this idea and to gain ready access to a broader range of materials, we developed a general synthesis of COPVs and examined their behavior upon positive doping and photoexcitation. We report here an efficient synthesis of higher oligomers of COPVs, their remarkably high stability as well as their polarons, bipolarons, and photoexcited states, and on the physicochemical evidence of strain-driven weakening of the vinylenic bonds. The COPV oligomers are far more stable under photolysis in air than that of the parent PVs and P3HT [poly(3-hexylthiophene)], which quickly decomposed under the same conditions. Unlike those of heteroatom-stabilized oligomers and polymers, the dication of COPV-6 is delocalized over the entire π -system and behaves as a bipolaron instead of a polaron pair.⁶

RESULTS AND DISCUSSION

Synthesis of COPVs. We synthesized COPV-*n* ($n = 3\text{--}6$) by an iterative synthetic strategy exploiting the one we

Received: September 20, 2012

Published: October 29, 2012

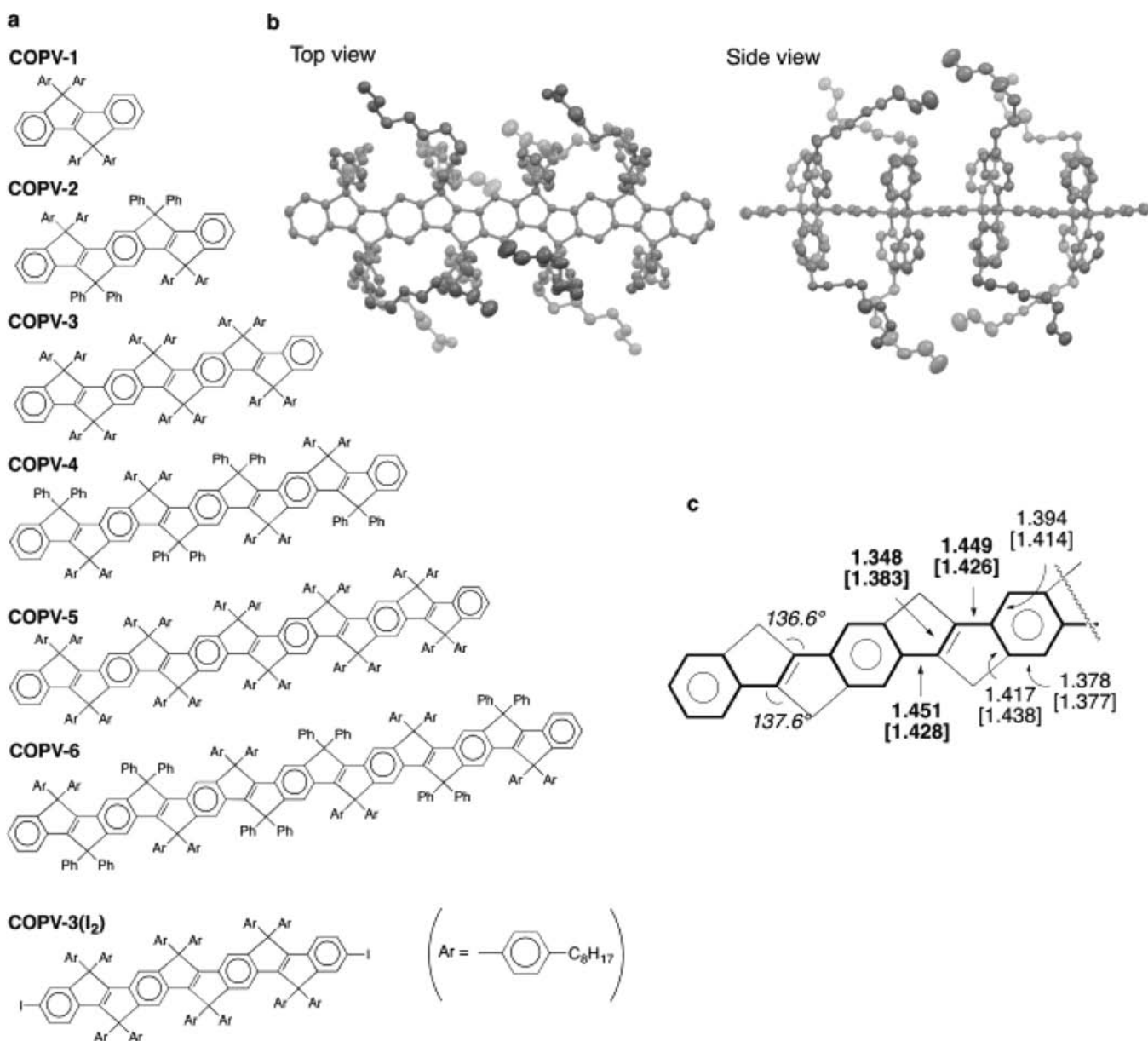


Figure 1. COPV-1–6 and COPV-4 cations. Ar = 4-octylphenyl. (a) Molecular structures. (b) Single-crystal X-ray analysis of COPV-4 (ORTEP drawing; 30% probability for thermal ellipsoid; hydrogen atoms, disordered component, and solvent atoms are omitted for clarity). (c) Representative structural data (in Å and °; substituents are omitted) of COPV-4 (X-ray), and [COPV-4]^{•+} (bracket; calculated at the UB3LYP/6-31G** level). The OPV skeleton is highlighted in bold. Upon one-electron oxidation, the vinylenic bond becomes shorter by 2.6%, and similarly the C–C bonds between the phenylene and vinylenic groups become slightly longer.

previously developed for COPV-1 and -2 (Supporting Information).⁴ Each step took place smoothly and reproducibly and produces versatile intermediates, such as COPV-3(I₂), that are useful for synthesizing longer oligomers, polymers, and other derivatives of COPVs. One PV unit is derived from one diarylacetylene and one arylmethanone unit. We incorporated several 4-octylphenyl groups to minimize intermolecular interactions (Figure 1b) and to enhance the solubility of the compounds. All compounds have C₂ symmetry, showed readily discernible NMR signals, and were further characterized by mass spectrometry and elemental analysis. COPV-6 has a molecular weight of 4007.89 and is 4.2 nm in length.

X-ray crystallographic structure of COPV-4 shows exceptionally large bond angles around the vinylenic carbon atoms, 136.6° and 137.6° (Figure 1c). Such large bond angles weaken

the vinylenic bonds, as revealed by the low Raman frequency of the double-bond stretching (see below). Nonetheless, the equilibrium bond length of 1.348 Å is rather close to the normal C=C double-bond length of 1.34 Å. The conjugated core of the molecule is slightly distorted from planarity because of either crystal packing or Jahn–Teller distortion (Figures 1b and S21a). The crystal structure illustrates the steric protection of the π -system by the 4-octylphenyl groups (Figure 1b), and in a single crystal, they separate each molecule far enough to avoid intermolecular interaction, as compared with nonbridged OPV-4⁷ (Figure S21b), and we consider that it is the case in solution and on the surface of a substrate.⁵

Stability. The most notable property of COPVs relevant to materials applications is high thermal and photochemical stability. COPVs can be kept on a shelf in air without

decomposition at least for one year. COPV-6 melts at 220 °C, and its TG-DTA analysis under nitrogen showed 5 wt % loss at 432 °C. Such stability of COPVs stands in contrast to the instability of unsubstituted PVs with several repeating units (>2).

Photostability is particularly important. COPV-4 survives photolysis at 30 °C with a half-life of 1578 min in air-saturated methylcyclohexane solution under illumination with a 300 W xenon lamp (intensity of ca. 1×10^6 W/m²). Comparison of the zero-order decay of the strongest absorption in the visible light region indicated that P3HT decomposes 8.3 times faster than COPV-4. Similarly, 1,4-bis[(*E*)-styryl]benzene decomposes over 100 times faster with a half-life of only 12 min. As discussed below, this stability originates from the lack of nonradiative decay of the singlet excited state of COPVs.

Absorption, Emission, and Electrochemical Properties of COPVs. The spectral properties support very effective conjugation in COPVs because of the rigid planar structure. UV-vis absorption spectra of the neutral COPVs exhibited intense, well-defined vibronic bands (ϵ up to 1.8×10^5 L/mol-cm, Figure 2a, and the top two rows of Table 1 together

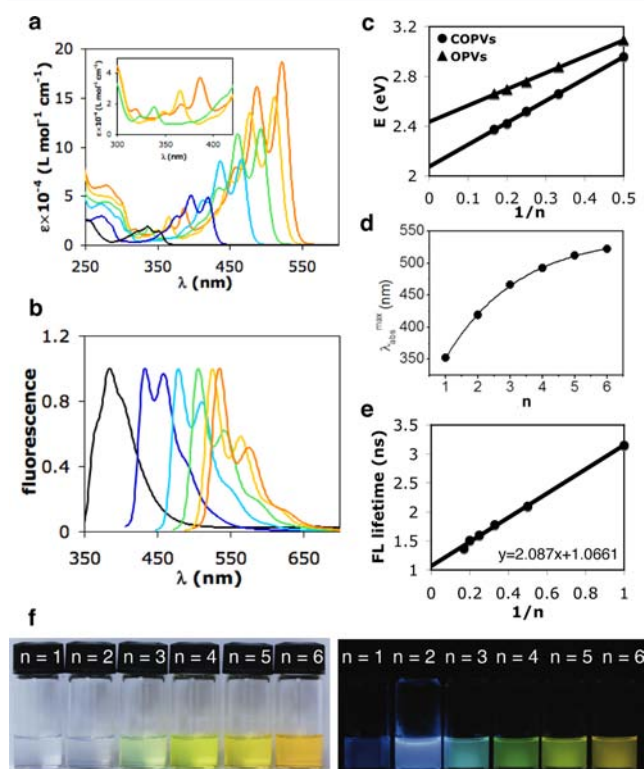


Figure 2. Spectral properties of COPV-1–6 in dichloromethane (ca. 10^{-6} M). (a) UV-vis absorption; (b) emission; (c) linear plot of transition energies against $1/n$; (d) exponential fits of absorption data of COPVs; and (e) linear plot of the fluorescence lifetimes vs the reciprocal of the number of COPV units (n). (f) Photographs of colors under room light and under 360 nm irradiation.

with the calculated absorption wavelengths) assignable to the HOMO \rightarrow LUMO ($S_0 \rightarrow S_1$) excitation (see Table S1). The colors are shown in Figure 2f.

As shown in Figure 2c, the plot of the 0–0 transition energy against the reciprocal number of repeating units ($1/n$, measured at 25 °C) showed an excellent linear correlation (Figure 2c, $R^2 = 0.9996$) with a slope of 1.76. The perfect linearity of the

correlation in turn indicates that the octyl group in the Ar group does not affect the transition energies of COPV framework, which is supported by the fact that COPV-1, bearing the Ar groups and its congener bearing four phenyl groups,^{4a} shows exactly the same UV-vis spectra. The slope⁸ is much larger than the value of 1.31 reported for OPVs (dipropoxy-substituted oligo(phenylenevinylene)s at 25 °C). Based on Meier's equation,⁹ the maximum absorption of an infinite chain (λ_∞) was determined to be 544 nm (Figure 3d), which is 63 nm longer than that of OPVs, and the maximum effective conjugation length is 13 PV units, which is larger than the value of 11 units reported for OPVs.

The photoluminescence properties of COPVs support the similarity of the structures between the ground and the excited states. The emission spectra are close to those of mirror images of the absorption spectra (Figure 2a vs 2b), proving that most of the intensity in the absorption bands is due to a single electronic transition (HOMO \rightarrow LUMO). The emission maximum wavelengths of COPVs are progressively longer (Figure 2b, and data in rows 3–6 of Table 1). Their Stokes shifts are very small and decrease progressively from 1309 to 501 cm^{-1} as n increases (Table 1, row 6), which are markedly smaller than those of OPVs (4036 to 2675 cm^{-1}). These values translate into reorganization energies ($\lambda(\text{M}/\text{M}^*)$) from 0.096 to 0.062 eV. The fluorescence quantum yields were almost unity irrespective of the chain length.¹⁰ The fluorescence lifetimes (τ) are 3.15–1.37 ns and are significantly longer than those of the corresponding OPVs, 0.62–0.25 ns.¹¹ The lifetimes of COPVs exhibit an excellent linear relationship with the reciprocal number of repeating units ($1/n$) (Figure 2e, $R^2 = 0.998$). These data indicate the absence of nonradiative decay pathways which are predominant for OPVs.

COPVs could be oxidized up to stable tetracations under cyclic voltammetric (CV) conditions (Table 1, row 8). COPV-1 shows one reversible oxidation process at 0.86 V (vs Fc^+/Fc) at scan rates between 25 and 400 $\text{mV}\cdot\text{s}^{-1}$ with the cathodic/anodic peak current ratios (i_a/i_c) equal to 1.0. The CV curves did not change after 50 cycles and up to a potential of 2.1 V without any electropolymerization. COPV-2 shows one reversible oxidative process at 0.53 V as opposed to the more difficult, irreversible oxidation of *E*-stilbene and 1,4-bis[(*E*)-styryl]benzene at 1.01 and 0.74 V, respectively. We recorded reversible two-electron oxidations for COPV-3 and COPV-4, and reversible three-electron oxidation for COPV-5. COPV-6 exhibited an unprecedented reversible four-electron oxidation waves at 0.18, 0.41, 0.76, and 0.98 V within the window of the tetrabutylammonium perchlorate/dichloromethane system. The reorganization energies $\lambda(\text{M}/\text{M}^+)$ (B3LYP and UB3LYP) calculated for COPV-2–6 are 0.237, 0.211, 0.190, 0.168, and 0.147 eV, respectively. These values are much smaller than nonbridged counterparts.¹² The value of $\lambda(\text{M}/\text{M}^+)$ for COPV-6, 0.147 eV, is similar to that for pentacene (ca. 0.100 eV).¹³

Absorption of Cationic COPVs. The high stability of the cations of COPVs¹⁴ allowed us, for the first time among heteroatom-free PV-type polymers and oligomers, to measure the spectra of the radical cation and the dication of a series of COPVs. We did not find any sign of decomposition of radical cations and dications during the measurements at room temperature.

A typical example is shown in Figure 3 for COPV-4, which was oxidized in degassed anhydrous dichloromethane by titration with a solution of one-electron oxidant, thianthrenium

Table 1. Photophysical and Electrochemical Properties of COPVs

properties	unit	COPV-1	COPV-2	COPV-3	COPV-4	COPV-5	COPV-6
λ_{abs}^a	nm	323, 336, 352	376, 396, 419	413, 437, 466	435, 461, 492 (338) ^b	450, 478, 512 (366) ^b	459, 488, 522 (387) ^b
$\epsilon \times 10^{-4c}$	cm ⁻¹ M ⁻¹	1.39	4.84	8.70	11.9	15.1	18.6
λ_{em}^d	nm	385	433, 458	479, 511	507, 542	526, 566	536, 575
Φ_F^e		0.98	1.00	1.00	1.00	1.00	1.00
τ^f	ns	3.15	2.10	1.78	1.60	1.51	1.37
Stokes shift	cm ⁻¹	1309	772	583	602	520	501
$\lambda(M/M^*)^g$	eV	—	0.096	0.072	0.075	0.064	0.062
$E_{\text{ox}}^{1/2h}$	V	0.86	0.53	0.32, 0.76	0.27, 0.60	0.17, 0.46, 0.94	0.18, 0.41, 0.76, 0.98
RC, λ_{abs}^a	nm	—	575, 640 1020, 1082	589, 648, 730, 1232, 1498	632, 705, 794, 1460, 1831	673, 752, 833, 1664, 2157	771, 862, 1818, 2445
DC, λ_{abs}^a	nm	—	—	946, 1078	1119, 1324	1329, 1628	1526, 1938

^aAbsorption maximum wavelengths of the neutral species, radical cations and dications measured in dichloromethane. ^bSubgap absorption. ^cExtinction coefficients for the most intense absorption band. ^dFluorescence maximum wavelengths measured in dichloromethane. ^eFluorescence quantum yield determined using absolute method. ^fFluorescence lifetime measured with the time-correlated single-photon counting operation mode. ^gReorganization energy between ground and excited states. ^hCV on a carbon electrode with Bu₄NClO₄ in dichloromethane (0.1 M, vs Fc⁺/Fc).

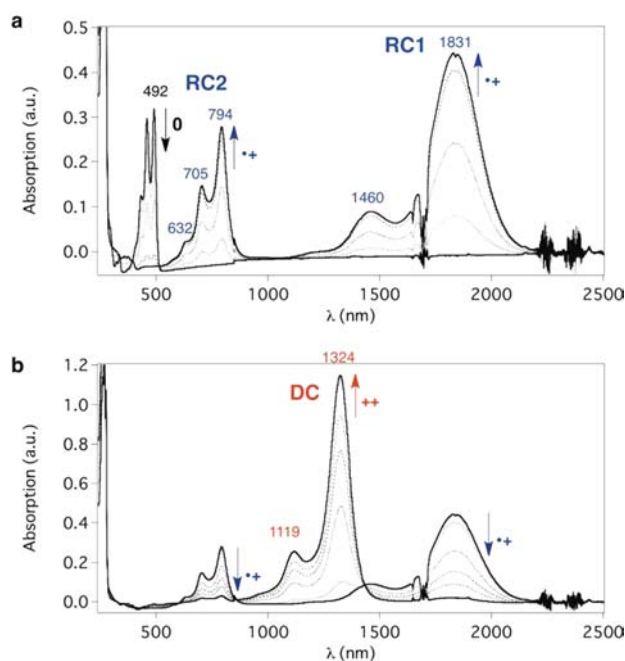


Figure 3. UV-vis NIR spectral titration of COPV-4 (2.68×10^{-6} M) in dichloromethane with the incremental addition of a solution of TH⁺ClO₄ to 2 equiv. (a) From neutral to radical cation; and (b) radical cation to dication.

perchlorate (TH⁺ClO₄, $E^0 = 0.76$ V vs Fc⁺/Fc) in a stepwise manner. Upon gradual addition of 1 equiv of oxidant, two subgap absorption bands resulting from a radical cation [COPV-4]^{•+} emerged at 794 nm (RC2 = radical cation band 2) and 1831 nm (RC1 band 1) with the disappearance of the 492 nm band from the neutral compound. This change occurred with an isosbestic point at 516 nm. The appearance of two bands at longer wavelength agrees with what one expects for a radical cation. Upon further addition of the oxidant up to 2 equiv, one new structured absorption band at 1324 nm (DC = dication band; [COPV-4]²⁺) appeared with the disappearance of the RC1 and RC2 bands. This change occurred with two isosbestic points at 860 and 1435 nm. The appearance of a single new DC band between the RC1 and RC2 bands agrees with the formation of a closed-shell dication.

The absorption data for the cations and dications compiled in Figure 4 and Table 1 (rows 9–10) showed excellent linear correlation between the transition energies of RC1 and RC2 and $1/n$ (Figure 4a). The low-energy RC1 bands are more sensitive to the size of the conjugation than the RC2 bands, which agree with the calculated data (Table S1). The maximum absorptions of the COPV dication (DC band) also showed a very good $1/n$ dependence on the transition energies. Notably, the planar framework of COPV here forces the two polarons (radical cations) to interact strongly with each other to form a bipolaron (dication). In conventional flexible conjugated systems, the system twists itself to leave two positive polarons out of conjugation, thus forming a polaron pair.¹⁵

Raman Analysis of Neutral and Positively Charged COPVs. The strain-driven activation of the ground state of COPV-3–6 is conclusively demonstrated by the Raman analysis of the neutral and cationic molecules. The analysis also highlights their unique electronic properties in which positive doping promotes electron redistribution within the rigid C=C/C–C core without much structural change.

The Raman spectra of the neutral compounds, COPV-1 to -6, in the solid state are shown Figure 5a. One conspicuous feature is a much smaller number of Raman bands than for conventional OPVs.¹⁶ In addition, the frequency and intensity pattern significantly change as n increases. This is ascribed to: (1) high local molecular symmetry of the conjugated core; (2) small influence of the lateral aryl substitution; and (3) effective electron–phonon coupling that enhances the Raman activity of those vibrations coupled to the electronic excitations, leaving unexcited molecular segments silent.¹⁷

We first compare COPV-2 with its analogue, (1,4-bis[(*E*)-3,5-di-*tert*-butylstyryl]benzene) (OPV-2). While OPV-2 shows three bands around 1630, 1590, and 1550 cm⁻¹, COPV-2 shows similar bands with a shift toward lower frequencies 1614 (black), 1596 (red), and 1543 cm⁻¹ (blue) as a result of more effective conjugation. The 1596 cm⁻¹ band is due to a collective CC stretching mode of the phenyl rings. This intense band for COPV-1–6 is rather insensitive to n , appearing at 1602, 1596, 1598, 1598, 1599, and 1598 cm⁻¹.

The Raman band (black) at 1617, 1614, 1586, 1587, 1582, and 1583 cm⁻¹ belongs to the collective stretching modes of the vinylene bonds and hence is most relevant to the present

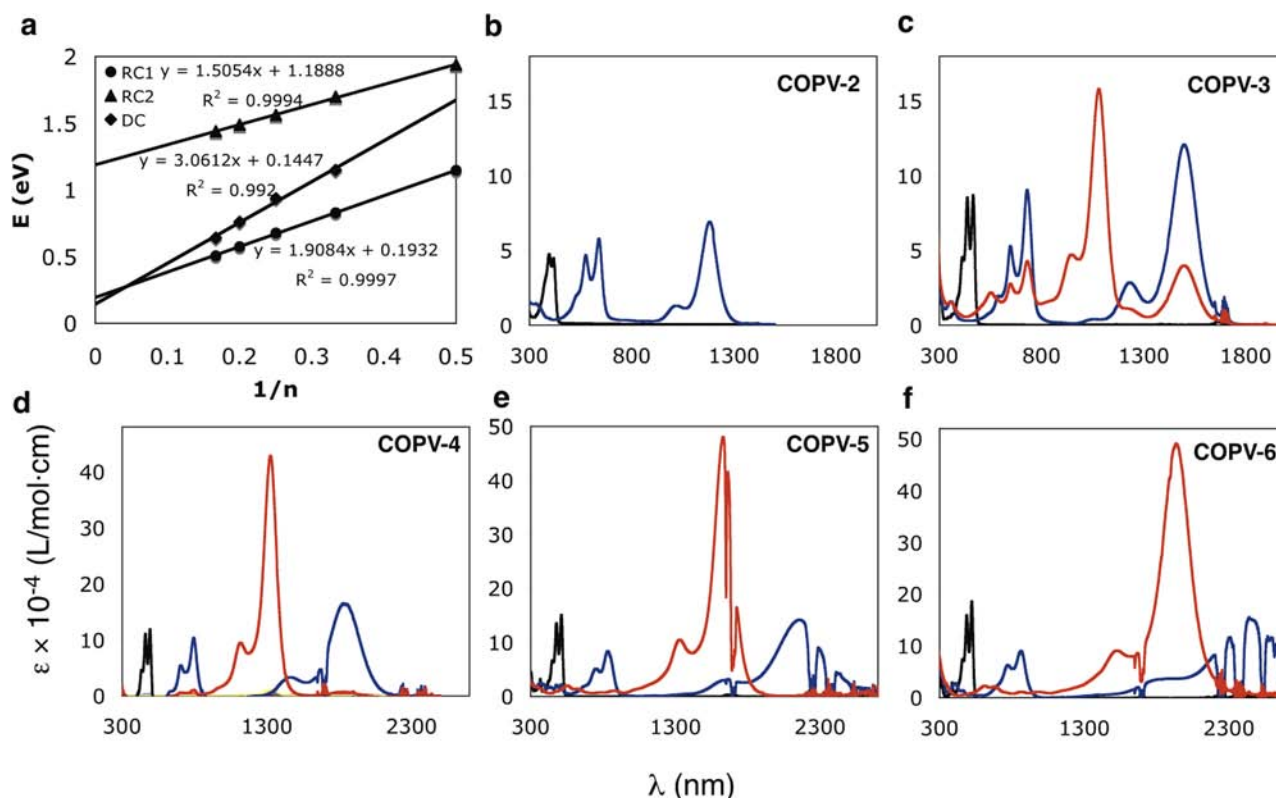


Figure 4. UV-vis NIR absorption spectra of neutral and positively charged COPVs in CH_2Cl_2 (black: neutral; blue: radical cation; red: dication). (a) Linear plot of transition energies against $1/n$ for the radical cation (RC1 and RC2 bands) and dication (DC) of COPV-4. (b–f) Spectra of neutral, radical cation, and dication of COPV-2–6.

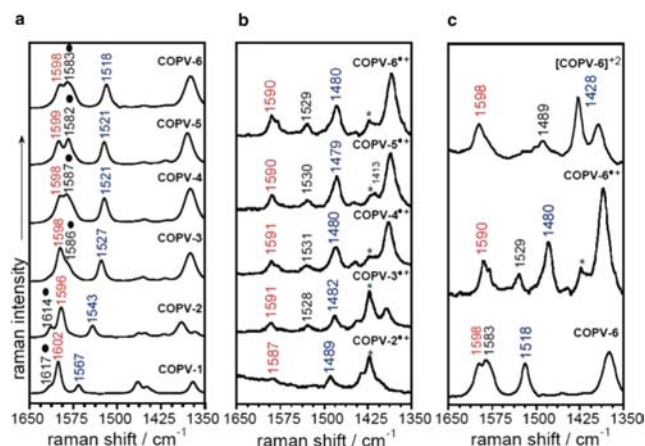


Figure 5. Raman spectra of COPV-1–6. (a) 1064 nm FT-Raman spectra of the COPV compounds in the solid state. (b) 532 nm resonant Raman spectrum of $[\text{COPV-2}]^{\bullet+}$ and 785 nm resonant Raman spectra of $[\text{COPV-3}]^{\bullet+}$, $[\text{COPV-4}]^{\bullet+}$, $[\text{COPV-5}]^{\bullet+}$, and $[\text{COPV-6}]^{\bullet+}$ in CH_2Cl_2 solutions (the asterisk denotes the Raman band of the solvent). (c) Absorption spectra of COPV-6 (black), $[\text{COPV-6}]^{\bullet+}$ (blue), and $[\text{COPV-6}]^{2+}$ (red). (d) 1064 nm FT-Raman spectrum of COPV-6, 785 nm resonant Raman spectrum of $[\text{COPV-6}]^{\bullet+}$, and 1064 nm FT-Raman spectrum of $[\text{COPV-6}]^{2+}$.

study. This band is very sensitive to n (by -34 cm^{-1} from COPV-1–6). This line weakens slightly from COPV-1 to -2 (by -3 cm^{-1}), and very much in COPV-3 (by -28 cm^{-1} COPV-2 to -3), in which the strained vinylenes are now flanked by two PV units on both sides. The conjugation effect saturates between COPV-3 and -6 (-4 cm^{-1} change). Note

that there is little change of the vinylene stretching frequency for conventional OPV.¹⁶

We assign the third band (blue) to a second collective CC stretching of the CC vinylene stretching modes coupled with the benzene vibrations. The Raman spectra show a large frequency downshift by -25 cm^{-1} from 1543 cm^{-1} in COPV-2 to 1518 cm^{-1} in COPV-6, but the conjugation effect saturates gradually toward COPV-3. From the behavior of the three characteristic bands, we conclude that it is not the benzene rings, but only the vinylene moiety that feels the ring strain of the bicyclo[3.3.0] ring, of which they are a part.

Figure 5b displays the resonance Raman spectra of the radical cations of five compounds ($[\text{COPV-2-6}]^{\bullet+}$). Comparison with the neutral spectra indicates that the vinylene bond weakens very much upon oxidation. As seen in the two vinylene stretching bands at ca. 1530 and 1480 cm^{-1} , the vinylene bonds are much weaker than those in the neutral compounds, whereas the benzene rings are insensitive (ca. 1590 cm^{-1}).

Figure 5c shows the Raman spectra of the stable dication $[\text{COPV-6}]^{2+}$ together with that of COPV-6 and $[\text{COPV-6}]^{\bullet+}$. The two vinylene stretching bands, 1583 and 1518 cm^{-1} in the neutral compound, shift down to 1529 and 1480 cm^{-1} in the radical cation and further to 1489 and 1428 cm^{-1} in the dication. In contrast, the benzene modes around 1600 cm^{-1} changed very little but broadened significantly, probably because of the formation of an extended quinoidal segment that encompasses seven benzene rings (Figure 1c). The Raman characteristics of the polaron and bipolaron indicate that the radical and cation are delocalized over the entire π -system of COPV-6. This interpretation is consistent with the effective conjugation number of 13 PV units.

CONCLUSION

We have developed an efficient synthesis of new heteroatom-free OPV derivatives (COPV-*n*) that are stable under photolysis in air and doped with very small reorganization energy to generate stable and fully delocalized positive polarons and bipolarons. Photoexcitation occurs with an extremely small reorganization energy. Both the ease of photoexcitation and the stability of the cations originate from the fact that the ground state is activated (or destabilized) by the bond angle strain associated with the bicyclo[3.3.0]octatriene rings. The Raman data indicated that the strain effects become particularly prominent for COPV-*n* larger than COPV-3, where the internal PV group(s) enjoys full conjugation with the two peripheral PV rings. The rigid and flat σ -framework provides efficient conjugation of the π -system up to 13 PV units and allows the formation of a bipolaron in COPV-6. The stable tetracation of COPV-6 observed under electrochemical oxidation is an interesting subject for more detailed studies in the future. In this vein, the well-defined structure and physical properties of COPVs make them ideal subjects for theoretical and physical studies. The present synthesis has made available useful synthetic building blocks, such as COPV-3(I₂), and will arouse interest in the changes of materials' properties created by replacement of the conventional PV and polythiophene derivatives in molecular wires¹⁸ and bulk organic optoelectronics materials.¹⁹ A positive indication has already been obtained for the monomer COPV-1 in the DSSC studies.

ASSOCIATED CONTENT

Supporting Information

Complete experimental details, CIF file of COPV-4. This material is available free of charge via the Internet at <http://pubs.acs.org>.

AUTHOR INFORMATION

Corresponding Author

tsuji@chem.s.u-tokyo.ac.jp; nakamura@chem.s.u-tokyo.ac.jp

Present Address

^{||}Organic Solids Laboratory, Beijing National Laboratory for Molecular Sciences, Institute of Chemistry, Chinese Academy of Sciences, Beijing 100190, P. R. China

Notes

The authors declare no competing financial interest.

ACKNOWLEDGMENTS

We thank MEXT for financial support (KAKENHI for E.N., no. 22000008, H.T., no. 20685005). This work was partly supported by a Grant-in-Aid for Scientific Research on Innovative Areas (for H.T., no. 23108704, " π -Space") from MEXT, Japan, and Masashi Maruyama for crystallographic analysis. J.T.L.N. and J.C. thank MEC (CTQ2009-10098) and Junta de Andalucía (PO9-4708). X.Z. thanks the JSPS Postdoctoral Fellowship for Foreign Researchers (no. P 09046).

REFERENCES

(1) Skotheim, T. A.; Reynolds, J. *Handbook of Conducting Polymers*, 2nd ed.; CRC press: New York, 1997.
(2) (a) Burroughes, J. H.; Bradley, D. D. C.; Brown, A. R.; Marks, R. N.; Mackay, K.; Friend, R. H.; Burns, P. L.; Holmes, A. B. *Nature* **1990**, *347*, 539–541. (b) Gustafsson, G.; Cao, Y.; Treacy, G. M.; Klavetter, F.; Colaneri, N.; Heeger, A. J. *Nature* **1992**, *357*, 477–479.

(c) Yu, G.; Gao, J.; Hummelen, J. C.; Wudl, F.; Heeger, A. J. *Science* **1995**, *270*, 1789–1791.

(3) (a) Grozema, F. C.; Candeias, L. P.; Swart, M.; van Duijnen, P. Th.; Wildeman, J.; Hadziioannou, G.; Siebbeles, L. D. A.; Warman, J. M. *J. Chem. Phys.* **2002**, *117*, 11366–11378. (b) Schwartz, B. J. *Nat. Mater.* **2008**, *7*, 427–428. (c) Meier, H. *Angew. Chem. Int., Ed. Engl.* **1992**, *31*, 1399–1420. (d) Waldeck, D. H. *Chem. Rev.* **1991**, *91*, 415–436. (e) Chambon, S.; Rivaton, A.; Gardette, J.-L.; Firon, M.; Lutsen, L. J. *Polym. Sci., Part A: Polym. Chem.* **2007**, *45*, 317–331.

(4) (a) Zhu, X.; Mitsui, C.; Tsuji, H.; Nakamura, E. *J. Am. Chem. Soc.* **2009**, *131*, 13596–13597. (b) Scherf, U.; Müllen, K. *Makromol. Chem., Rapid Commun.* **1991**, *12*, 489–497.

(5) Zhu, X.; Tsuji, H.; Yella, A.; Chauvin, A.-S.; Grätzel, M.; Nakamura, E. *Chem. Commun.*, submitted.

(6) Cornil, J.; Beljonne, D.; Brédas, J. L. *J. Chem. Phys.* **1995**, *103*, 834–841 and references therein.

(7) van Hutten, P. F.; Wildeman, J.; Meetsma, A.; Hadziioannou, G. *J. Am. Chem. Soc.* **1999**, *127*, 5910–5918.

(8) (a) Bidan, G.; De Nicola, A.; Enée, V.; Guillerez, S. *Chem. Mater.* **1998**, *10*, 1052–1058. (b) Izumi, T.; Kobashi, S.; Takimiya, K.; Aso, Y.; Otsubo, T. *J. Am. Chem. Soc.* **2003**, *125*, 5286–5287.

(9) (a) Stalmach, U.; Kolshorn, H.; Brehm, I.; Meier, H. *Liebigs Ann.* **1996**, 1449–1456. (b) Meier, H.; Stalmach, U.; Kolshorn, H. *Acta Polym.* **1997**, *48*, 379–384.

(10) Hsu, J.-H.; Hayashi, M.-t.; Lin, S.-H.; Fann, W.; Rothberg, L. J.; Perng, G.-Y.; Chen, S.-A. *J. Phys. Chem. B* **2002**, *106*, 8582–8586.

(11) Peeters, E.; Ramos, A. M.; Meskers, S. C. J.; Janssen, R. A. J. *J. Chem. Phys.* **2000**, *112*, 9445–9454.

(12) Liu, D.; Yin, S.; Xu, H.; Liu, X.; Sun, G.; Xie, Z.; Yang, B.; Ma, Y. *Chem. Phys.* **2011**, *388*, 69–77.

(13) Deng, W.-Q.; Goddard, W. A., III *J. Phys. Chem. B* **2004**, *108*, 8614–8621.

(14) van Hal, P. A.; Beckers, E. H. A.; Peeters, E.; Apperloo, J. J.; Janssen, R. A. J. *Chem. Phys. Lett.* **2000**, *328*, 403–408.

(15) González, S.; Ie, Y.; Aso, Y.; Navarrete, J. T. L.; Casado, J. *J. Am. Chem. Soc.* **2001**, *123*, 16350–16353 and references therein.

(16) Tian, B.; Zerbi, G.; Schenk, R.; Müllen, K. *J. Chem. Phys.* **1991**, *95*, 3191–3197.

(17) Zerbi, G.; Galbiati, E.; Gallazzi, M. C.; Castiglioni, C.; del Zoppo, M. *J. Chem. Phys.* **1996**, *105*, 2509–2516.

(18) Diez-Perez, I.; Hihath, J.; Hines, T.; Wang, Z.-S.; Zhou, G.; Müllen, K.; Tao, N. *Nat. Nanotechnol.* **2011**, *6*, 226–231.

(19) (a) Hagfeldt, A.; Boschloo, G.; Sun, L.; Kloo, L.; Pettersson, H. *Chem. Rev.* **2010**, *110*, 6595–6663. (b) Li, C.; Liu, M.; Pschirer, N. G.; Baumgarten, M.; Müllen, K. *Chem. Rev.* **2010**, *110*, 6817–6855. (c) van Hutten, P. F.; Krasnikov, V. V.; Hadziioannou, G. *Acc. Chem. Res.* **1999**, *32*, 257–265. (d) Song, S.; Jin, Y.; Kim, S. H.; Moon, J.; Kim, K.; Kim, J. Y.; Park, S. H.; Lee, K.; Suh, H. *Macromolecules* **2008**, *41*, 7296–7305.